

Redox-Regulated Lipid Membrane Binding of the PICK1 PDZ Domain^{†,‡}

Yawei Shi,*§,||,⊥ Jiang Yu,^{||,⊥} Yuan Jia,[§] Lifeng Pan,^{||} Chong Shen,^{||} Jun Xia,^{||} and Mingjie Zhang*,||

[§]Institute of Biotechnology, Shanxi University, Taiyuan, P. R. China, and ^{||}Department of Biochemistry, Molecular Neuroscience Center, State Key Laboratory of Molecular Neuroscience, Hong Kong University of Science and Technology, Kowloon, Hong Kong, P. R. China. [⊥]These authors contributed equally to this work.

Received February 23, 2010; Revised Manuscript Received April 27, 2010

ABSTRACT: PICK1 is a PDZ/BAR domain-containing scaffold protein that regulates the trafficking of many receptors and ion channels, including AMPA receptors. In addition to binding to a wide spectrum of target proteins to be transported, the PICK1 PDZ domain, via its conserved CPC motif, has also been shown to bind to lipid membranes. However, the molecular basis of the CPC motif-mediated lipid membrane binding of the PICK1 PDZ domain is not known. Here we show that the Cys residues in the CPC motif of the PICK1 PDZ domain forms reversible, intermolecular disulfide bonds under mild oxidation conditions. Importantly, formation of the disulfide-mediated dimer abolishes the lipid membrane binding capacity of the PICK1 PDZ domain and thereby is expected to alter the cellular functions of PICK1. The structures of the PDZ dimers provide atomic-scale pictures of disulfide-mediated PICK1 dimer formation and a molecular explanation of the oxidation-induced dissociation of PICK1 from membranes. We propose that the PICK1-mediated trafficking processes might be regulated by cellular redox fluctuations under both physiological and pathophysiological conditions.

PICK1,¹ originally identified as a protein interacting with kinase 1 (*I*), is now known to interact with a large number of transmembrane receptors and ion channels (*2*). PICK1 contains two well-conserved domains (an N-terminal PDZ domain and a C-terminal BAR domain) and serves as an adaptor in linking receptors and ion channels to vesicular trafficking machinery. The PDZ domain of PICK1 is responsible for binding to the majority of receptors and ion channels embedded in the trafficking vesicles (*2, 3*). The BAR domain of PICK1, by forming a homodimer or a heterodimer with the BAR domain of ICA69, is believed to anchor PICK1 to various vesicular or plasma membranes (*4, 5*). The best studied PICK1-mediated receptor/ion channel trafficking system would be AMPA receptors. Direct

binding of the GluR2 C-terminal tail to the PDZ domain of PICK1 is required for targeting AMPA receptors to synapses (*6–10*). In addition to GluR2, PICK1, via its PDZ domain-mediated binding, is also implicated in the trafficking of metabotropic glutamate receptors (*11–14*). *PICK1* knockout mice are deficient in AMPA receptor trafficking, and mutant mice lack cerebellar long-term depression (*15*).

In addition to binding to the carboxyl tail peptides of receptors and ion channels being transported, the PDZ domain of PICK1 has also been demonstrated to bind to lipid membranes (*16*). The PDZ domain–membrane interaction requires a highly conserved “⁴⁴CysProCys⁴⁶” motif (termed the CPC motif) located in the βB–βC loop as well as a positively charged surface opposite the target peptide binding groove of the PICK1 PDZ domain. Mutations of individual or both Cys residues in the CPC motif abolished the lipid binding capacity of the PICK1 PDZ domain, and the same mutations had a negligible impact on the GluR2 binding of the domain (*16*). In stark contrast to the wild-type protein, PICK1 containing a PDZ domain lipid binding-deficient mutation (both Cys44 and Cys46 substituted with Gly) is completely diffused in neurons and the mutant PICK1 is impaired in both clustering and synaptic targeting of AMPA receptors (*16*), although the exact role of the two Cys residues in the PICK1’s membrane binding is unclear. This study, together with the BAR domain–lipid membrane interaction studies (*4, 5*), indicated that the lipid binding capacities of both the PDZ domain and the BAR domain are critical for PICK1-mediated receptor/ion channel trafficking and membrane localizations. However, it is not known whether and how the PDZ domain-mediated lipid membrane binding of PICK1 might be regulated.

PDZ domain–membrane interactions are increasingly being recognized as a general property of a large subset of PDZ domains in the mammalian genomes (*17*). Compared to that of the extensively studied PDZ–protein interactions, the biochemical

[†]Supported by grants from the Research Grants Council of Hong Kong to M.Z. (HKUST663407, 663808, 664009, CA07/08.SC01, SEG_HKUST06, and AoE/B-15/01-II) and the National Science Foundation of Shanxi Province (2007021033), the National Science Foundation of China (30400065), and the Key project of the Chinese Ministry of Education (208020) to Y.S.

[‡]The coordinates of the wild-type PICK1 PDZ dimer and the C46G mutant PDZ dimer have been deposited in the Protein Data Bank as entries 3HPK and 3HPM, respectively.

*To whom correspondence should be addressed. M.Z.: Department of Biochemistry, Hong Kong University of Science and Technology, Clear Water Bay, Kowloon, Hong Kong; e-mail, mzhang@ust.hk. Y.S.: Institute of Biotechnology, Shanxi University, Taiyuan, P. R. China; e-mail, yaweishi@sxu.edu.cn; phone, 852-2358-8709; fax, 852-2358-1552.

[§]Abbreviations: AMPAR, α-amino-3-hydroxy-5-methylisoxazole-4-propionic acid receptor; BAR, Bin/amphiphysin/Rvs; DTT, d,L-1,4-dithiothreitol; FITC, fluorescein 5-isothiocyanate; GluR2, glutamate receptor 2; HEPES, 4-(2-hydroxyethyl)-1-piperazineethanesulfonic acid; NEM, *N*-ethylmaleimide; NMDA, *N*-methyl-D-aspartic acid; PICK1, protein interacting with c kinase 1; ICA69, islet cell autoantigen of 69 kDa; PDZ, post-synaptic density protein (PSD-95), Disc large (Dlg), and Zonula occludens-1 (ZO-1); PMSF, phenylmethanesulfonyl fluoride; PEG3350, polyethylene glycol 3350; rmsd, root-mean-square deviation; SDS-PAGE, sodium dodecyl sulfate–polyacrylamide gel electrophoresis.

and structural basis of PDZ–lipid membrane interactions is poorly understood.

In this work, we discover that the Cys residues in the CPC motif of the PICK PDZ domain can be specifically oxidized to form intermolecular disulfide bonds under mild oxidative conditions. Most importantly, formation of inter-PDZ disulfide bonds abolishes the lipid membrane binding capacity of the domain, suggesting that redox-mediated PDZ oxidation could be used as a molecular mechanism in regulating PICK1 clustering and target trafficking. The structures of disulfide-mediated PICK1 PDZ dimers determined here provide molecular insights into oxidation-mediated PICK1 covalent dimer formation.

MATERIALS AND METHODS

Protein Expression and Purification. The preparation of the PICK1 PDZ domain (residues 18–110) or its mutants fused with the nine C-terminal amino acid residues of the GluR2 subunit (VYGIESVKI) of the AMPA receptors was described previously (16). For the ligand-free PICK1 PDZ domain, the C-terminal GluR2 tail was cleaved with 3C protease and removed when the digested mixture was passed through several cycles of Sephadryl S-200 gel filtration chromatography using a column buffer containing 50 mM Tris-HCl (pH 7.5), 100 mM NaCl, and 10 mM DTT.

Ligand Binding Affinity Determined by Fluorescence Spectroscopy. Fluorescence spectra were recorded on a Perkin-Elmer LS-55 fluorescence spectrophotometer equipped with a polarizer at 25 °C. Fluorescence titration was performed via addition of an increasing amount of reduced or oxidized of PICK1 PDZ domain to a constant concentration of an N-terminal FITC-labeled GluR2 tail peptide (~0.5 μM) in 20 mM HEPES buffer containing 100 mM NaCl (pH 7.4). The titration curves were fitted with MicroCal Origin.

Analytical Gel Filtration Chromatography. Analytical gel filtration chromatography was conducted on an AKTA FPLC system (GE Healthcare). Proteins or protein mixtures were analyzed using a Superose 12 10/300 GL column (GE Healthcare) with the column buffer containing 50 mM Tris-HCl and 100 mM NaCl, with or without 10 mM DTT (pH 7.5).

Analytical Ultracentrifugation. Sedimentation velocity experiments were performed on a Beckman XL-I analytical ultracentrifuge equipped with an eight-cell rotor at 42000 rpm and 25 °C. The partial specific volume of individual protein sample and the buffer density were calculated using SEDNTERP (<http://www.rasmb.bbri.org/>). The sedimentation velocity data of the PICK1 PDZ domain in the presence or absence of DTT were analyzed and fitted to a continuous sedimentation coefficient distribution model, with the fitting result shown as solid lines using SEDFIT (<http://www.analyticalultracentrifugation.com/default.htm>).

Lipid Binding Assay. Brain lipid extracts (Folch fraction I, Sigma B1502) were freshly prepared in a buffer containing 20 mM HEPES (pH 7.4) and 150 mM NaCl (16). The protein sample (5 μM) was incubated with 0.5 mg/mL liposomes in 40 μL of buffer for 15 min at room temperature and then spun at 80000g for 15 min at 4 °C in a Beckman TLA100.1 rotor. The supernatants were removed for the determination of the amount of proteins not bound to liposomes. The pellets were washed twice with the same buffer and resuspended with 40 μL of the same buffer. The supernatant and the pellet proteins were subjected to reducing or nonreducing SDS-PAGE and visualized by Coomassie blue staining.

Cell Culture and DNA Transfection, with Western Blot Analysis. Human embryonic kidney (HEK293) cells were cultured in Dulbecco's modified essential medium supplemented with 10% fetal bovine serum, 100 units/mL penicillin G, 100 μg/mL streptomycin, and 0.25 μg/mL amphotericin B at 37 °C. Cells were seeded onto six-well plates and transfected with the myc-tagged wild-type full-length PICK1 or its C44G, C46G, or C44,46G mutant expression construct individually using lipofectamine transfection reagents (Invitrogen). Approximately forty-eight hours post-transfection, HEK293 cells were treated with 1 mM H₂O₂ for 15 min before being harvested. Cells were lysed using a lysis buffer composed of 20 mM Tris-HCl (pH 7.5), 150 mM NaCl, 1% Triton X-100, 0.5% NP-40, 1 mM EDTA, and 1 mM PMSF. The free sulphydryl groups of proteins were blocked via addition of 20 mM *N*-ethylmaleimide (NEM) to the cell lysates, and the mixture was incubated on ice for 30 min. The proteins in the cell lysates were separated by 8% SDS-PAGE without reducing agent. PICK1 was detected by Western blot analysis using an anti-myc antibody (from Invitrogen).

Crystallization of the Dimeric PICK1 PDZ Domain. The C46G mutant of the PICK1 PDZ domain (3.0 mg/mL) was treated with 1 mM H₂O₂ for 20 min at room temperature. The resulted dimeric PDZ was separated from the unreacted monomer by gel filtration chromatography. Crystals were grown with dimeric C46G-PDZ domain (10 mg/mL) in 20 mM Tris-HCl and 100 mM NaCl (pH 7.5) using the hanging-drop method by mixing 1 μL of protein sample with an equal volume of 20% (w/v) PEG4000 and 0.1 M HEPES (pH 7.5) at 16 °C. The wild-type PICK1 PDZ domain [10 mg/mL in 20 mM Tris-HCl, containing 100 mM NaCl and 1 mM DTT (pH 7.5)] was crystallized by mixing 1 μL of protein sample with an equal volume of precipitant composed of 20% (w/v) PEG3350 and 0.2 M lithium citrate (pH 8.4) at 16 °C. Crystals appeared ~5 months after the drop setting.

Determination of the Structure. Crystals were transferred to the reservoir solution containing 10% (v/v) glycerol as the cryoprotectant and flash-cooled with liquid nitrogen. Diffraction data were collected at 110 K on a Rigaku RAXIS IV⁺⁺ imaging plate system with a MicroMax-007 copper rotating anode generator. The diffraction data were processed and scaled using MOSFLM (18) and SCALa in the CCP4 suite (19).

The oxidized dimeric PICK1 PDZ structures were determined by the molecular replacement method with Phaser (20) using the solution structure of the monomeric PICK1 PDZ domain [Protein Data Bank (PDB) entry 2PKU] as the search model (16). Structures were fitted and rebuilt with Coot (21) and refined with REFMAC5 (22) and CNS (23). The overall qualities of the structural models were assessed using PROCHECK (24). Data collection and refinement statistics are listed in Table 1.

RESULTS

The PDZ Domain of PICK1 Tends To Form a Disulfide-Mediated Dimer in Solution. In our earlier structural studies of the PICK1 PDZ domain, we discovered that inclusion of freshly prepared DTT (> 5 mM) in the buffer was necessary to keep the protein in the reduced and monomeric form (16). Analytical gel filtration chromatography analysis of the PICK1 PDZ domain in the DTT-free buffer revealed a monomer–dimer equilibrium (Figure 1A, blue curve). The dimer population of the PICK1 PDZ domain increased progressively if the protein sample was left in the DTT-free buffer for a longer period of

Table 1: Data Collection and Refinement Statistics for the Structures of the C46G-PICK1 and Wild-Type PDZ Dimers

	C46G mutant	wild type
Data Collection		
space group	$P2_12_12_1$	$P2_12_12_1$
unit cell dimensions	$a = 37.45 \text{ \AA}$, $b = 54.00 \text{ \AA}$, $c = 92.38 \text{ \AA}$ $\alpha = \beta = \gamma = 90^\circ$	$a = 49.26 \text{ \AA}$, $b = 51.79 \text{ \AA}$, $c = 80.83 \text{ \AA}$ $\alpha = \beta = \gamma = 90^\circ$
resolution (\AA)	46.62–2.80 (2.95–2.80) ^a	80.85–2.20 (2.32–2.20) ^a
no. of observed reflections	20938	101296
no. of unique reflections	4797	11020
R_{merge}^b (%)	6.4 (37.7) ^a	6.7 (41.7) ^a
I/σ	7.6 (2.0) ^a	10.3 (1.8) ^a
average redundancy	4.4 (4.4) ^a	9.2 (9.1) ^a
completeness (%)	96.8 (96.8) ^a	99.9 (99.9) ^a
Refinement		
resolution (\AA)	46.62–2.80 (2.872–2.800) ^a	80.85–2.20 (2.257–2.200) ^a
$R_{\text{work}}^c/R_{\text{free}}^d$ (last shell)	24.3/29.5 (30.1/38.8)	20.6/23.5 (22.2/29.4)
mean B factor (\AA^2)	53.5	32.3
rmsd		
bond lengths (\AA)	0.009	0.009
bond angles (deg)	1.310	1.124
Ramachandran plot (residues, %)		
most favored	90.3	92.1
additionally allowed	9.7	7.3
generously allowed	0	0.6

^aThe values in parentheses refer to the highest-resolution shell. ^b $R_{\text{merge}} = \sum_h \sum_i |I_i h(\ln)| / \sum_h |I_h|$, where (I_h) is the mean intensity of i observations of reflection h . ^c $R_{\text{factor}} = \sum_h |F_{\text{obs}}| - |F_{\text{calc}}| / \sum_h |F_{\text{obs}}|$, where F_{obs} and F_{calc} are the observed and calculated structure factor amplitudes, respectively. Summation includes all reflections used in the refinement. ^d $R_{\text{free}} = \sum_h |F_{\text{obs}}| - |F_{\text{calc}}| / \sum_h |F_{\text{obs}}|$, evaluated for a randomly chosen subset of 10% of the diffraction data not included in the refinement.

time, and the protein could be converted into a near-complete dimer when the sample was left in the DTT-free buffer for ~ 5 h (Figure 1A, red and black curves). We next performed an *in vitro* H_2O_2 -mediated oxidation analysis of the PICK1 PDZ domain. Exposure of the fully reduced PICK1 PDZ domain (prepared by collecting the monomeric protein peak via preparative gel filtration chromatography) to moderate concentrations of H_2O_2 (< 1 mM) led to accelerated, H_2O_2 concentration-dependent PDZ dimer formation (Figure 1B). This disulfide-mediated PDZ dimer can be fully converted back to the monomer via addition of sufficiently high concentrations of DTT [> 10 mM (Figure 1C)]. We further analyzed the monomer–dimer equilibrium of the PICK1 PDZ domain in buffer containing different concentrations of DTT using the sedimentation velocity analysis method. In the absence of DTT, the PICK1 PDZ domain was shown as one broad peak, presumably representing the coalesced monomer and dimer peaks with comparable volumes (Figure 1D). Addition of DTT shifted the equilibrium of the PDZ domain toward the monomer population. A significant PICK1 PDZ dimer population (~10%) could still be observed even when 2 mM DTT was included in the sample buffer (Figure 1D). Taken together, the biochemical studies described here indicate that the PICK1 PDZ domain has an intrinsic propensity to form a disulfide-mediated dimer under mild oxidation conditions.

We next compared the backbone $^1\text{H}-^{15}\text{N}$ HSQC NMR spectra of the PICK1 PDZ domain in its reduced (black peaks) and oxidized (red) forms (Figure 1E). Disulfide-mediated oxidation led to severe broadening of a large proportion of backbone amide peaks of the PICK1 PDZ domain. By taking advantage of the chemical shift assignments of the reduced form of the protein (16), we were able to map the oxidation-induced peak broadening of the domain. It is clear that the residues that

undergo the oxidation-induced peak broadening are located in the “⁴⁴CPC⁴⁶” motif and its vicinity regions of the domain (Figure 1F). The PICK1 PDZ domain contains only two Cys residues, and both Cys residues are in the CPC motif of the domain. The CPC motif is strictly conserved in PICK1 from different species (16). The two Cys residues were shown to be absolutely required for the PICK1 PDZ domain to bind to lipid membranes, and both Cys residues of the CPC motif were required for the formation of PICK1 clusters *in vivo* and for PICK1-mediated AMPA receptor trafficking in neurons (16). However, the molecular basis of CPC motif-dependent membrane association of the PICK1 PDZ domain was not known. Additionally, it was not clear how PICK1 PDZ domain–lipid membrane interaction is regulated. The biochemical and biophysical data shown in Figure 1 suggest that oxidation of the Cys residues in the CPC motif of the PDZ domain might be used as a regulatory switch in controlling PICK1-mediated receptor/ion channel trafficking.

Formation of the PICK1 PDZ Dimer First Occurs via the Intermolecular Cys44–Cys44' Disulfide Bond. Since the PICK1 PDZ domain forms a specific intermolecular disulfide-mediated dimer under mild oxidation conditions, one or both of the Cys residues in the CPC motif (Cys44 and Cys46) must be involved in the formation of the disulfide bond(s). We tried to determine which of the two Cys residues is more susceptible to oxidation. First, we compared the analytical gel filtration profiles of the wild-type PICK1 PDZ domain and its C44G, C46G, and C44,46G mutants [single or double Cys to Gly mutants (see ref 16)]. As one would expect, the C44,46G mutant of the PICK1 PDZ domain eluted as a single monomer peak, as the mutant protein is free of SH groups (Figure 2A). We noted that the C44G mutant of the PICK1 PDZ domain also eluted as a near-complete

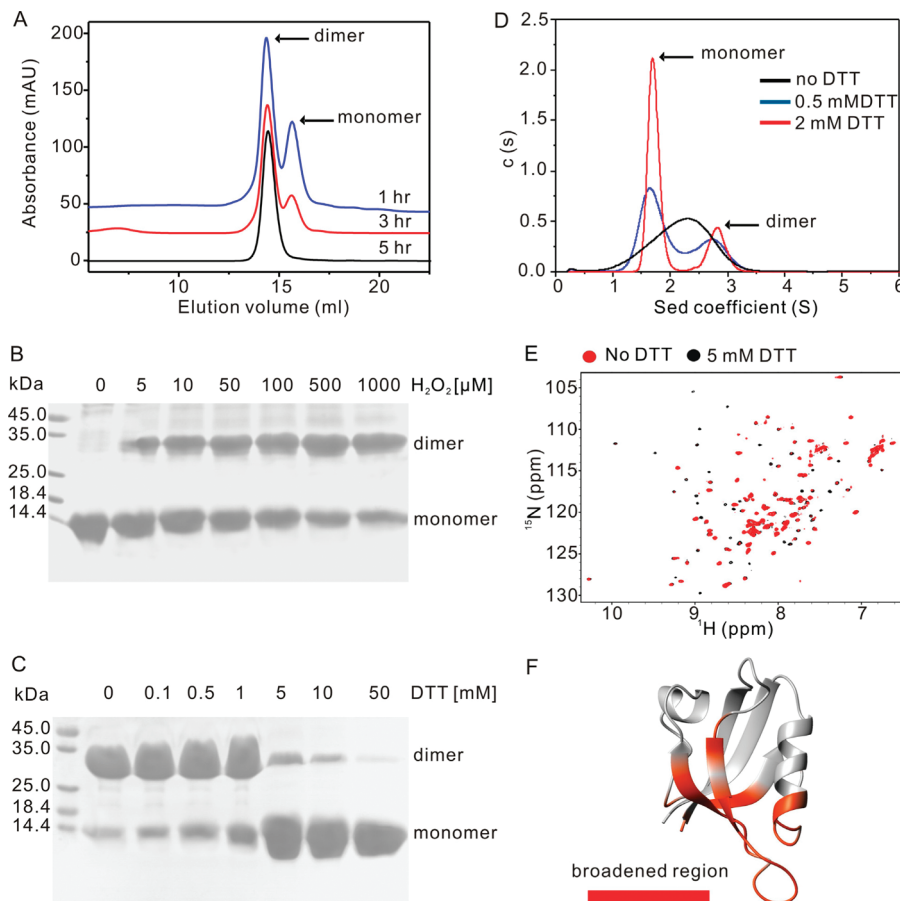


FIGURE 1: Disulfide bond-mediated dimerization of the PICK1 PDZ domain. (A) The PICK1 PDZ domain can be oxidized to a dimer by being exposed to air oxygen when analyzed on an analytical gel filtration column. Exposing the DTT-free protein sample (4 mg/mL) to air for 5 h led to near-complete oxidation of the domain. (B) Nonreducing SDS-PAGE analysis of the oxidation of the PICK1 PDZ domain with increasing concentrations of H_2O_2 . In this reaction, the PICK1 PDZ domain (2.6 mg/mL) in 50 mM Tris-HCl buffer containing 100 mM NaCl and 1 mM EDTA (pH 7.5) was incubated with the indicated concentrations of H_2O_2 for 30 min at 25 °C before being loaded on the SDS-PAGE gel. (C) Nonreducing SDS-PAGE analysis showing that the oxidized PICK1 PDZ dimer can be converted into a monomer by addition of DTT. (D) Sedimentation velocity analysis of the PICK1 PDZ domain (2 mg/mL) in the presence of various concentrations of DTT in the sample buffer. (E) Superposition plot of the ^1H - ^{15}N HSQC spectra of the PICK1 PDZ domain with or without 5 mM DTT in the sample buffer, showing large chemical shift changes of the domain upon oxidation. (F) Mapping of the oxidation-induced backbone amide peak broadenings of the PICK1 PDZ domain onto its three-dimensional structure. The regions of the domain colored red represent the residues that undergo oxidation-induced broadening.

monomer (Figure 2A), indicating that Cys44 of the PDZ domain is more susceptible to oxidation-induced disulfide bond formation. Consistent with this observation, the C46G mutant of the PDZ domain had an elution profile similar to that of the wild-type protein [i.e., the protein displayed an obvious monomer–dimer equilibrium (Figures 1A and 2A)]. On nonreducing SDS-PAGE, the C44G mutant had a lower population of dimer when compared to the wild type and the C46G mutant and C44,46G ran as a single monomer band (Figure 2B,C). Again, the disulfide-mediated dimer formation of the C44G and C46G mutants of the PICK1 PDZ domain is reversible upon addition of DTT to the SDS-PAGE sample buffer (Figure 2B). Finally, the C44G mutant of the PICK1 PDZ domain exhibited a weaker tendency to form H_2O_2 -induced dimer compared to the wild-type and C46G mutant of the PICK1 PDZ domain (Figure 2D). Taken together, these biochemical analyses showed that Cys44 in the CPC motif of the PICK1 PDZ domain undergoes oxidation-induced disulfide bond formation first and Cys46 is relatively more inert to oxidation.

Oxidation-Mediated Dimerization Abolishes the Lipid Membrane Binding Capacity of the PICK1 PDZ Domain. We showed previously, using site-directed mutagenesis approaches,

that the Cys residues in the CPC motif are absolutely required for the binding of the PICK1 PDZ domain to lipid membranes in vitro and for the formation of PICK1 clusters in vivo (16). We reasoned that the formation of oxidation-induced intermolecular disulfide bonds of the PICK1 PDZ1 domain would disrupt the lipid membrane binding property of the domain, thereby providing a potential regulatory switch for the PICK1 PDZ domain–membrane interaction. To test this hypothesis, we prepared the pure dimeric and monomeric forms of the PICK1 PDZ domain by passing the domain through a preparative gel filtration column. The obtained monomer and dimer proteins were immediately subjected to a sedimentation-based liposome binding assay (16). In the absence of brain liposomes, neither the monomeric nor the dimeric PICK1 PDZ domain was precipitated in the centrifugation-based assay (Figure 3A,B). The monomeric PICK1 PDZ domain exhibited specific binding to lipid liposomes (Figure 3A). In contrast, the dimeric PICK1 PDZ domain exhibited no liposome binding in the same assay (Figure 3B,C). The biochemical data given above indicate that the lipid membrane binding capacity of the PICK1 PDZ domain (and hence the clustering and target trafficking property of PICK1) can be regulated by oxidation of Cys residues

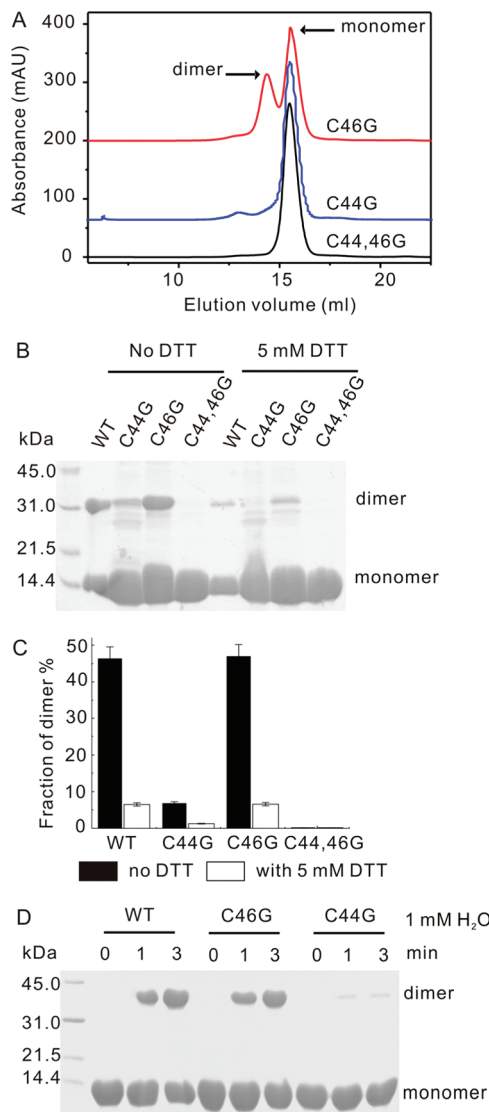


FIGURE 2: Cys44 of the PICK1 PDZ domain is more susceptible to oxidation. (A) Analytical gel filtration analysis of the oxidation profiles of the C44G, C46G, and C44,46G mutants of the PICK1 PDZ domain. (B) Nonreducing SDS–PAGE analysis of the oxidation properties of the wild-type PICK1 PDZ domain and its mutants. The figure shows that both the wild-type and C46G mutant forms of the PICK1 PDZ domain formed a significant portion of dimer when the monomeric proteins were exposed to air for 120 min. The figure also shows that the disulfide-mediated PICK1 PDZ dimers could be converted into monomers if the sample was treated with 5 mM DTT before SDS–PAGE analysis. (C) Quantification of the percentage of the dimeric PICK1 PDZ domain and its mutants with or without 5 mM DTT. Values are means \pm the standard deviation of three different experiments. (D) Cys44 in the PICK1 PDZ domain is more susceptible to H₂O₂-induced oxidation. In this experiment, the monomeric PICK1 PDZ domain and its mutants (1.5 mg/mL) were first incubated with 0.5 mM H₂O₂ for different periods of time before nonreducing SDS–PAGE analysis.

in its CPC motif in vitro. Given that the Cys residues of the PICK1 PDZ domain (Cys44 in particular) can be oxidized under relatively mild oxidation conditions, we hypothesize that the reversible, oxidation-mediated PICK1 dimerization might be employed as a molecular mechanism in regulating PICK1 cluster formation and/or dispersion in vivo. However, future studies are required to test this hypothesis.

To obtain an atomic-scale picture of the oxidation-mediated dimerization of the PICK1 PDZ domain, we tried to crystallize

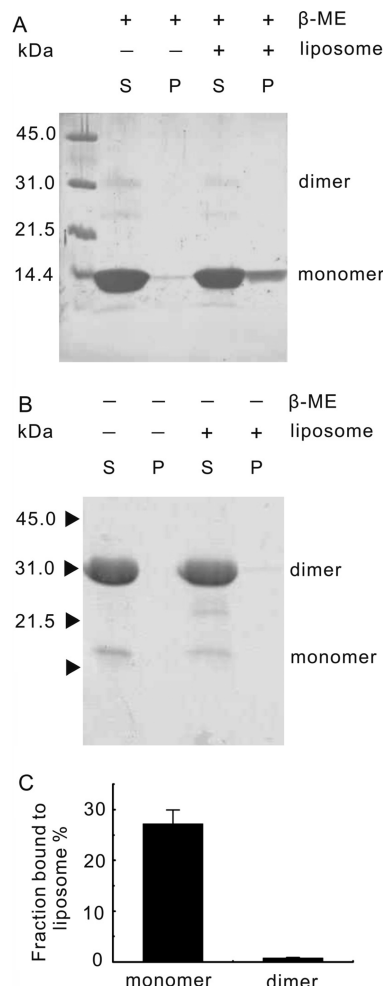


FIGURE 3: Formation of the disulfide-mediated dimer abolishes the lipid membrane binding capacity of the PICK1 PDZ domain. (A) Sedimentation-based liposome binding assay showing that the reduced monomeric PICK1 PDZ domain binds to lipid membranes. (B) The oxidized PICK1 PDZ dimer no longer binds to lipid membranes. In this figure, S and P denote proteins recovered in the supernatant and pellet, respectively, of the assay mixture after ultracentrifugation. β -Mercaptoethanol (2 mM) was included in the monomeric PICK1 PDZ domain to keep the protein in its reduced form. (C) Quantification of interactions between liposomes and the dimeric or monomeric PICK1 PDZ domain. Values are means \pm standard deviation obtained from three different experiments.

the PDZ dimer. To simplify potential nonspecific oxidation, we used the C46G mutant of the PICK1 PDZ domain for crystallization trials on the basis of the following two reasons. First, the C46G mutant displays an oxidation profile similar to that of the wild-type protein (Figures 1 and 2). Second, the wild-type PICK1 PDZ domain failed to crystallize \sim 4–5 weeks after the crystallization drops had been set up. In contrast, crystals of the C46G mutant matured within 2 days, and crystals diffracted to 2.8 Å resolution in an in-house diffractor. We determined the structure of the C46G mutant of the PICK1 PDZ domain by the molecular replacement method using the reduced monomeric PDZ domain structure as the search model (Figure 4A). As expected, Cys44 in the C46G mutant forms an intermolecular disulfide bond (Figure 4B), and the two PDZ domains contact each other via the bottom face of the domain (with respect to the target-binding α B– β B groove). The overall conformation of the PDZ domain, in the reduced monomer or the oxidized dimer, is essentially the same (rmsd of 0.62 Å for the main chain atoms). The noticeable

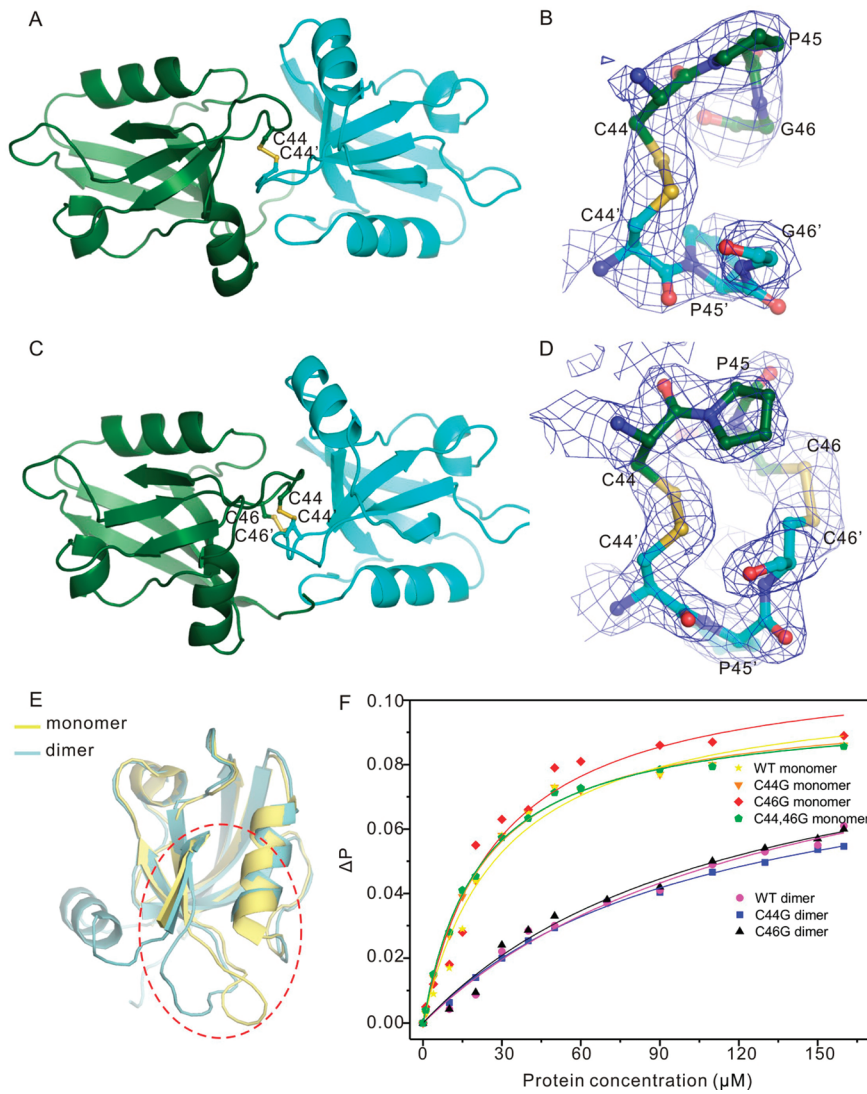


FIGURE 4: Structures of the oxidized PICK1 PDZ dimers. (A) Ribbon diagram representation of the dimeric C46G mutant of the PICK1 PDZ domain. The intermolecular disulfide bond formed by Cys44 from two PDZ molecules is drawn using an explicit atomic model. (B) Molecular details of the inter-PDZ domain disulfide bond formed in the C46G PDZ dimer. Electron densities are contoured at 1.0σ . (C) Ribbon diagram representation of the wild-type PICK1 PDZ dimer. (D) Molecular details of the inter-PDZ domain disulfide bonds formed in the wild-type PDZ dimer. Electron densities are also contoured at 1.0σ . (E) Comparison of the overall conformations of the wild-type PICK1 PDZ domain in its reduced monomer form (yellow) and oxidized dimer form (sky blue). The obvious conformational difference in the β B– β C loop between the two forms of the PICK1 PDZ domain is highlighted. (F) Formation of dimer decreases the GluR2 peptide binding affinities of the PICK1 PDZ domain and its mutants.

difference of the two forms is in the β B– β C loop of the PDZ domain (see below for more details). To our surprise and delight, the wild-type PICK1 PDZ domain crystal in the presence of 1 mM DTT appeared \sim 5 months after the crystal drops had been set up, and the crystals diffracted to 2.2 Å (Table 1). The structure, again determined by the molecular replacement method using the monomeric PICK PDZ domain structure as the search model, showed that the wild-type PICK1 PDZ domain contains two disulfide bonds, formed via intermolecular Cys44–Cys44' and Cys46–Cys46' pairing (Figure 4C,D). The Cys44–Cys44' disulfide bond, both in the C46G mutant and in the wild-type PDZ domain, adopts a near-optimal disulfide bond geometry with a right-handed spiral configuration with a $\text{Ca}–\text{Ca}'$ distance of 5.71 Å. The Cys46–Cys46' disulfide bond adopts the left-handed staple conformation with a $\text{Ca}–\text{Ca}'$ distance of 6.24 Å (25). The dihedral strain energy is in the range of 14.0–16.2 kJ/mol for the right-handed spiral Cys44–Cys44' disulfide bond and 18.9–24.8 kJ/mol for the right-handed spiral

Cys46–Cys46' disulfide bond (18), showing that the Cys44–Cys44' disulfide bond is more stable than the Cys46–Cys46' disulfide bond. Furthermore, Cys44 is located at the center of the β B– β C loop of the PDZ domain and more accessible to oxidants than Cys46 which is located at the start of β C. The three-dimensional structure of the wild type and the C46G mutant PICK1 PDZ dimer structures, together with the biochemical data shown in Figures 1 and 2, firmly establish that Cys44 of the PICK1 PDZ domain is oxidized first to form an intermolecular Cys44–Cys44' disulfide bond. Subsequently, two Cys46 residues, brought into the proximity of the Cys44–Cys44' bond-mediated PDZ dimer, can slowly form another pair of disulfide bonds. Again, the overall conformation of the wild-type PDZ domain in the oxidized dimer is essentially the same as that in the monomer (an rmsd of 0.54 Å). The only noticeable difference is in the β B– β C loop of the domain (Figure 4E). Upon formation of intermolecular disulfide bonds, the β B– β C loop moves \sim 7 Å away from the α B helix (Figure 4E), and this conformational

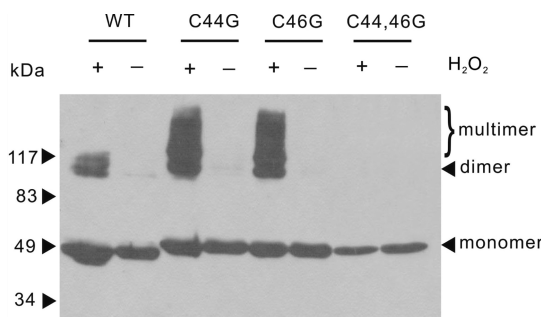


FIGURE 5: Full-length PICK1 can form the disulfide-mediated covalent dimer under oxidative stress in vivo. The figure shows that wild-type, myc-tagged PICK1 and its C44G and C46G mutants (probed with an anti-myc antibody) can form the disulfide-mediated dimer as well as the multimer when cells were treated with mild oxidation stress.

change is correlated with significantly weakened GluR2 tail peptide binding of the oxidized PDZ domain (Figure 4F; the peptide binding affinity of the monomeric PICK1 PDZ domain and its mutants is $\sim 25 \mu\text{M}$, whereas the dimeric forms have a decreased affinity of $\sim 130 \mu\text{M}$ in their K_d values). The GluR2 peptide binding data also imply that oxidation-mediated dimer formation of the PICK1 PDZ domain may also contribute to the AMPA receptor trafficking by directly modulating the PICK1–AMPAR interaction in addition to the PICK1 PDZ domain's membrane binding. Importantly, the structures of the two PICK1 PDZ dimers shown in panels A and C of Figure 4A also clearly explain the oxidation-induced loss of the lipid membrane binding of the PICK1 PDZ domain, as the membrane-penetrating CPC motif in the reduced PDZ monomer is buried in the interface of the oxidized dimer.

Full-Length PICK1 Can Form a Disulfide-Mediated Dimer under Oxidation Stress. We next investigated whether formation of the oxidation-induced intermolecular disulfide bond could occur for full-length PICK1 in living cells. To test this possibility, we individually overexpressed myc-tagged, wild-type full-length PICK1 and its C44G, C46G, and C44,46G mutants in HEK293 cells. The PICK1-expressing cells were treated with a low dose of H₂O₂ (1 mM) for 15 min before being harvested. The free sulphydryl groups of PICK1 in the cell lysates were blocked with *N*-ethylmaleimide. The resulting proteins were separated by nonreducing SDS-PAGE, and PICK1 was detected with an anti-myc antibody (Figure 5). Wild-type PICK1 exhibited specific covalent dimer bands only when cells were exposed to H₂O₂. In contrast, the C44,46G mutant of PICK1 showed no detectable dimer (or multimer) band, regardless of whether the cells were treated with H₂O₂, indicating the dimer band detected in wild-type PICK1 is mediated by the intermolecular disulfide bond(s) formed by Cys44 (and possibly Cys46 as well). Both the C44G and C46G mutants of PICK1 showed oxidation-dependent PICK1 dimer formation. We noted that the C44G and C46G mutants of PICK1 formed multimers as well under the oxidation conditions, and both mutants are more susceptible to oxidation-induced dimer (and multimer) formation than the wild-type protein (Figure 5). It is possible that mutation of an individual Cys residue led to dissociation of PICK1 from the membrane bilayers in the living cells (16) and, thus, exposure of the remaining Cys to the solvent to be readily oxidized by H₂O₂. The data presented in Figure 5 provide biochemical support that PICK1 has the possibility of undergoing oxidation-dependent, disulfide-mediated dimerization in living cells,

thereby affecting PICK1 clustering and PICK1-mediated target trafficking. It should be pointed out that the oxidation-mediated PICK1 dimerization or oligomerization in living cells is likely to be more complicated than in its isolated PDZ domain as the BAR domain of PICK1 is a membrane binding domain. Further work is required for detailed characterization of the full-length PICK1 oxidation both in vitro and in vivo. We noted that the C44G and C46G mutants of full-length PICK1 formed similar levels of dimer as well as oligomers when HEK293 cells were treated with H₂O₂ (Figure 5) even though Cys44 in the isolated PDZ domain is more susceptible to oxidation (Figure 2), further indicating that the BAR domain of PICK1 is also likely to influence the multimerization and oxidation properties of PICK1.

DISCUSSION

PICK1 is intimately linked to the trafficking of glutamate receptors (2). Both NMDA and AMPA types of glutamate receptors are well-known to be involved in neuronal excitotoxicity. Excessive overactivation of glutamate receptors leads to increased and sustained Ca²⁺ concentration elevation which leads to accumulation of cellular oxidants, including nitric oxide, peroxide, and other reactive oxygen species (26–28). The most common target for the cellular oxidants is Cys residues in proteins (29, 30). Upon reacting with oxidants such as H₂O₂, free sulphydryl groups from Cys residues can be oxidized into sulfenic, sulfenic, or sulfonic acids. Two Cys sulfenic groups can further form a reversible disulfide bond if they are in the proximity of each other (31). Such reactive oxidant-mediated Cys oxidations are known to be closely linked to cellular signaling events as well as oxidative damage-related pathologies (30, 31). Here, we discovered that the key AMPA receptor trafficking adaptor PICK1 can undergo oxidation-induced covalent dimerization via Cys residues in its PDZ domain in vitro. Such oxidation-induced dimerization of PICK1 might be used as a regulatory mechanism in dispersing PICK1 clusters in synapses (16), thereby controlling synaptic densities of PICK1-mediated receptors and ion channels including AMPA receptors. Interestingly, recent work showed that H₂O₂ can transiently increase to a high concentration beneath membrane bilayers by inactivating H₂O₂ detoxification of the enzyme peroxiredoxin (32). Given that PICK1 is a well-known membrane-associated protein, it is possible that transient increase in the level of H₂O₂ under certain cellular conditions can lead to oxidation-induced dimerization and declustering. It should be noted that the results presented in this study provide only a biochemical basis for potential redox-mediated PICK1 dimerization and subsequent declustering. Whether and how (if the answer to the first question is yes) such a mechanism operates in living cells are critical questions for future studies.

ACKNOWLEDGMENT

We thank Dr. Yanxiang Zhao for making the X-ray machine available for this study.

REFERENCES

1. Staudinger, J., Zhou, J., Burgess, R., Elledge, S. J., and Olson, E. N. (1995) PICK1: A perinuclear binding protein and substrate for protein kinase C isolated by the yeast two-hybrid system. *J. Cell Biol.* 128, 263–271.
2. Xu, J., and Xia, J. (2007) Structure and Function of PICK1. *Neurosignals* 15, 190–201.
3. Hanley, J. G. (2008) PICK1: A multi-talented modulator of AMPA receptor trafficking. *Pharmacol. Ther.* 118, 152–160.

4. Jin, W., Ge, W. P., Xu, J., Cao, M., Peng, L., Yung, W., Liao, D., Duan, S., Zhang, M., and Xia, J. (2006) Lipid binding regulates synaptic targeting of PICK1, AMPA receptor trafficking, and synaptic plasticity. *J. Neurosci.* **26**, 2380–2390.
5. Cao, M., Xu, J., Shen, C., Kam, C., Huganir, R. L., and Xia, J. (2007) PICK1-ICA69 heteromeric BAR domain complex regulates synaptic targeting and surface expression of AMPA receptors. *J. Neurosci.* **27**, 12945–12956.
6. Dev, K. K., Nishimune, A., Henley, J. M., and Nakanishi, S. (1999) The protein kinase C α binding protein PICK1 interacts with short but not long form alternative splice variants of AMPA receptor subunits. *Neuropharmacology* **38**, 635–644.
7. Xia, J., Zhang, X., Staudinger, J., and Huganir, R. L. (1999) Clustering of AMPA receptors by the synaptic PDZ domain-containing protein PICK1. *Neuron* **22**, 179–187.
8. Perez, J. L., Khatri, L., Chang, C., Srivastava, S., Osten, P., and Ziff, E. B. (2001) PICK1 Targets Activated Protein Kinase C α to AMPA Receptor Clusters in Spines of Hippocampal Neurons and Reduces Surface Levels of the AMPA-Type Glutamate Receptor Subunit 2. *J. Neurosci.* **21**, 5417–5428.
9. Kim, C. H., Chung, H. J., Lee, H. K., and Huganir, R. L. (2001) Interaction of the AMPA receptor subunit GluR2/3 with PDZ domains regulates hippocampal long-term depression. *Proc. Natl. Acad. Sci. U.S.A.* **98**, 11725–11730.
10. Terashima, A., Cotton, L., Dev, K. K., Meyer, G., Zaman, S., Duprat, F., Henley, J. M., Collingridge, G. L., and Isaac, J. T. (2004) Regulation of synaptic strength and AMPA receptor subunit composition by PICK1. *J. Neurosci.* **24**, 5381–5390.
11. Bertaso, F., Zhang, C., Scheschonka, A., de Bock, F., Fontanaud, P., Marin, P., Huganir, R. L., Betz, H., Bockaert, J., Fagni, L., and Lerner-Natoli, M. (2008) PICK1 uncoupling from mGluR7a causes absence-like seizures. *Nat. Neurosci.* **11**, 940–948.
12. Jo, J., Heon, S., Kim, M. J., Son, G. H., Park, Y., Henley, J. M., Weiss, J. L., Sheng, M., Collingridge, G. L., and Cho, K. (2008) Metabotropic glutamate receptor-mediated LTD involves two interacting Ca $^{2+}$ sensors, NCS-1 and PICK1. *Neuron* **60**, 1095–1111.
13. Suh, Y. H., Pelkey, K. A., Lavezzi, G., Roche, P. A., Huganir, R. L., McBain, C. J., and Roche, K. W. (2008) Corequirement of PICK1 binding and PKC phosphorylation for stable surface expression of the metabotropic glutamate receptor mGluR7. *Neuron* **58**, 736–748.
14. Zhang, C. S., Bertaso, F., Eulenburg, V., Lerner-Natoli, M., Herin, G. A., Bauer, L., Bockaert, J., Fagni, L., Betz, H., and Scheschonka, A. (2008) Knock-in mice lacking the PDZ-ligand motif of mGluR7a show impaired PKC-dependent autoinhibition of glutamate release, spatial working memory deficits, and increased susceptibility to pentylenetetrazol. *J. Neurosci.* **28**, 8604–8614.
15. Steinberg, J. P., Takamiya, K., Shen, Y., Xia, J., Rubio, M. E., Yu, S., Jin, W., Thomas, G. M., Linden, D. J., and Huganir, R. L. (2006) Targeted in vivo mutations of the AMPA receptor subunit GluR2 and its interacting protein PICK1 eliminate cerebellar long-term depression. *Neuron* **49**, 845–860.
16. Pan, L., Wu, H., Shen, C., Shi, Y., Jin, W., Xia, J., and Zhang, M. (2007) Clustering and synaptic targeting of PICK1 requires direct interaction between the PDZ domain and lipid membranes. *EMBO J.* **26**, 4576–4587.
17. Wu, H., Feng, W., Chen, J., Chan, L. N., Huang, S., and Zhang, M. (2007) PDZ domains of Par-3 as potential phosphoinositide signaling integrators. *Mol. Cell* **28**, 886–898.
18. Leslie, A. G. W. (1992) Recent changes to the MOSFLM package for processing film and image plate data. Joint CCP4+ESF-EAMCB Newsletter on Protein Crystallography, No. 26.
19. Collaborative Computational Project Numer 4 (1994) The CCP4 Suite: Programs for protein crystallography. *Acta Crystallogr. D50*, 760–763.
20. McCoy, A. J., Grosse-Kunstleve, R. W., Adams, P. D., Winn, M. D., Storoni, L. C., and Read, R. J. (2007) Phaser crystallographic software. *J. Appl. Crystallogr.* **40**, 658–674.
21. Emsley, P., and Cowtan, K. (2004) Coot: Model-building tools for molecular graphics. *Acta Crystallogr. D60*, 2126–2132.
22. Murshudov, G. N., Vagin, A. A., and Dodson, E. J. (1997) Refinement of macromolecular structures by the maximum-likelihood method. *Acta Crystallogr. D53*, 240–255.
23. Brunger, A. T., Adams, P. D., Clore, G. M., DeLano, W. L., Gros, P., Grosse-Kunstleve, R. W., Jiang, J. S., Kuszewski, J., Nilges, M., Pannu, N. S., Read, R. J., Rice, L. M., Simonson, T., and Warren, G. L. (1998) Crystallography & NMR system: A new software suite for macromolecular structure determination. *Acta Crystallogr. D54*, 905–921.
24. Laskowski, R. A., Moss, D. S., and Thornton, J. M. (1993) Main-chain bond lengths and bond angles in protein structures. *J. Mol. Biol.* **231**, 1049–1067.
25. Schmidt, B., Ho, L., and Hogg, P. J. (2006) Allosteric disulfide bonds. *Biochemistry* **45**, 7429–7433.
26. Carriedo, S. G., Sensi, S. L., Yin, H. Z., and Weiss, J. H. (2000) AMPA exposures induce mitochondrial Ca $^{2+}$ overload and ROS generation in spinal motor neurons in vitro. *J. Neurosci.* **20**, 240–250.
27. Sattler, R., Xiong, Z., Lu, W. Y., Hafner, M., MacDonald, J. F., and Tymianski, M. (1999) Specific coupling of NMDA receptor activation to nitric oxide neurotoxicity by PSD-95 protein. *Science* **284**, 1845–1848.
28. Forder, J. P., and Tymianski, M. (2009) Postsynaptic mechanisms of excitotoxicity: Involvement of postsynaptic density proteins, radicals, and oxidant molecules. *Neuroscience* **158**, 293–300.
29. Lambeth, J. D. (2004) NOX enzymes and the biology of reactive oxygen. *Nat. Rev. Immunol.* **4**, 181–189.
30. Rhee, S. G. (2006) Cell signaling. H $_2$ O $_2$, a necessary evil for cell signaling. *Science* **312**, 1882–1883.
31. Saurin, A. T., Neubert, H., Brennan, J. P., and Eaton, P. (2004) Wide spread sulfenic acid formation in tissues in response to hydrogen peroxide. *Proc. Natl. Acad. Sci. U.S.A.* **101**, 17982–17987.
32. Woo, H. A., Yim, S. H., Shin, D. H., Kang, D., Yu, D. Y., and Rhee, S. G. (2010) *Cell* **140**, 517–528.